ELSEVIER

Journal of Power Sources 84 (1999) 75–79

JOURNAL OF POWER SOURCES

www.elsevier.com/locate/jpowsour

Nickel-stabilized composite manganese oxides as lithium insertion electrodes

P. Lavela [a], L. Sánchez [a], J.L. Tirado [a,*], S. Bach [b], J.P. Pereira-Ramos [b]

[a] *Laboratorio de Química Inorgánica. Facultad de Ciencias. Universidad de Córdoba, Avda. San Alberto Magno s / n. 14004, Córdoba, Spain*
[b] *Laboratoire d'Electrochimie, Catalyse et Synthèse Organique, LECSO-CNRS UMR 7582, 2 Rue Henri Dunant, 94320 Thiais, France*

Received 14 March 1999; received in revised form 27 May 1999; accepted 22 June 1999

Abstract

The introduction of nickel atoms in Chemical Manganese Dioxide (CMD) is studied as an alternative route for the stabilization of the structure of these solids. X-ray diffraction data evidence the incorporation of nickel in different proportions in the poorly crystalline β/γ-MnO_2 structure of these materials. Step Potential Electrochemical Spectroscopy (SPES) of lithium anode cells using the nickel-modified solids as cathode material shows a significant improvement in the electrochemical performance upon cycling.

Keywords: Nickel atom; Chemical manganese dioxide; Lithium insertion electrode

1. Introduction

It is well known that the solid state chemistry of manganese oxides is particularly rich, due to the structural diversity and the different oxidation states in which manganese can occur. As a result, many solids belonging to the structural families of manganese oxides have been tested as lithium insertion electrodes for advanced lithium and lithium-ion cells [1]. However, success is restricted to two main groups of compounds: γ- and β-MnO_2 related solids [*chemical manganese dioxide* (CMD), and *electrochemical manganese dioxide* (EMD)] and spinel-structure $LiMn_2O_4$ and related compositions. The former were directly involved in the first commercial Li/manganese oxide rechargeable systems developed by Sony [2] and Sanyo [3]. Following these studies, it was shown that the thermal treatment of the dioxides with LiOH at 375°C allowed to incorporate some lithium in the structure, thus improving significantly the cycling properties of the electrodes [4–6]. The resulting materials were named CDMO (*Composite Dimensional Manganese Oxide*). The formation of layered Li_2MnO_3 should be avoided during lithium modification by limiting the temperature of thermal treatment, as the discharge behaviour of this solid is particularly poor. If the thermal treatment with LiOH is carried out at higher temperatures (500–600°C), a mixture of $LiMn_2O_4$ and Mn_2O_3 is obtained, from which the spinel shows a better cycling behaviour.

Here we present the improvement of the electrochemical behaviour of a composite manganese oxide without lithium by allowing the introduction of nickel by the carbonate precursor method. This method has been shown to be particularly useful in the preparation of mixed Mn–Co and Mn–Fe spinels [7], as well as spinel related Li–Mn–Co [8]. The behaviour of the resulting electrodes is also discussed.

2. Experimental

The mixed nickel manganese carbonate precursors with $Ni/(Ni + Mn) = 0.03$, 0.08 and 0.160 were prepared by the addition of a 1 M solution of $NaHCO_3$ to a 0.5 M solution of the divalent ions Ni^{2+} and Mn^{2+} under a continuous flow of CO_2. The nickel–oxide products were obtained by heating mixed carbonate precursors at 400°C in static air atmosphere during different periods from 1 to 24 h. The stoichiometry was confirmed by energy dispersive X-ray microanalysis coupled to a *JEOL JSM6300* scanning electron microscope. The XRD data were performed on a Siemens D-5000 X-ray diffractometer using

* Corresponding author. Tel.: +34-957-218637; fax: +34-957-218606; E-mail: iq1ticoj@lucano.uco.es

0378-7753/99/$ - see front matter
PII: S0378-7753(99)00304-3

CuK_α radiation and graphite monochromator. Thermogravimetric analysis was carried out with a Cahn 2000 electrobalance under dynamic argon and static air atmosphere.

The average oxidation state of metal ions in the sample was determined by the following procedure. About 20 mg of sample was dissolved in 5 ml of 0.1 M Fe^{2+} in 0.01 M H_2SO_4 under continuous flow of argon and heated until complete dissolution. The solution was titrated with standard 0.001 M $KMnO_4$. Previously the $KMnO_4$ solution was normalized with $Na_2C_2O_4$. The titrations were assigned to the excess of Fe^{2+} ions in the sample dissolution and used to calculate the oxygen to metal (O/M) ratios.

Electrochemical studies were carried out in two-electrode cells. The electrolyte used was 1 M $LiClO_4$, previously dried under vacuum at 170°C for 16 h, dissolved in distilled ethylene/propylene carbonate (1:1 mixture). The oxide electrode pellets (7 mm diameter) were prepared by pressing at 4 ton ca. 3 mg of active material with PTFE (5% w), graphite (7.5% w) and acetylene black (7.5% w) on a steel grid. Lithium foil was cut as 7 mm diameter circles and was used as the anode vs. the spinel oxide electrode. Unless otherwise specified, the cells were cycled at C/5 rate, which was controlled by a MacPile II potentiostat–galvanostat. Step potential electrochemical spectroscopy (SPES) spectra were recorded with 1 mV steps of one-hour duration.

3. Results and discussion

Three samples with different composition were prepared by varying the nickel content in the precursor. The solids will be henceforth referred to as samples A — $Ni_{0.03}Mn_{0.97}O_{1.67}$, B — $Ni_{0.08}Mn_{0.92}O_{1.61}$ and C — $Ni_{0.16}Mn_{0.84}O_{1.63}$, as obtained by chemical analysis of the oxide products. Thermogravimetric data obtained by allowing the complete reduction of the oxide to MO in a dynamic argon atmosphere were in excellent agreement with the chemical titration of the average oxidation state of manganese ions in the samples (A: 3.38, B: 3.33 and C: 3.5). It should be noted that the composition always showed an O/M ratio lower than 2 and slightly higher than to the intermediate M_5O_8 ratio. A clear evolution of the O/M ratio with nickel content is not observed and the differences between samples are never marked. In the evaluation of the average oxidation state of manganese ions, a Ni^{2+} oxidation state was assumed. This assumption is based in conclusions reported for other related mixed oxides. Thus, the XPS measurements reported by Amine et al. [9] confirmed clearly the +II oxidation state of nickel in $LiMn_{1.5}Ni_{0.5}O_4$. Other authors [10–12] also found the presence of Ni^{2+} in doped $LiMn_2O_4$ spinel oxides. For the lithium-free spinel $NiMn_2O_4$, Ni^{2+} is also found [13]. The experimentally determined compositions imply that the average oxidation state of manganese is particularly high for the higher nickel content (sample C).

Fig. 1 shows the X-ray diffraction patterns of the three pristine samples. Due to the enhanced broadening of the line profiles, a refinement of the unit cell parameters in a single phase was not successful. If the diffraction patterns are compared with those reported in the literature, a particular similarity is observed with that reported by Nohma et al. [1] for γ/β-MnO_2. An additional effect shown in Fig. 1 is the displacement to larger diffraction angles of some of the peak, as nickel content increases. This can be interpreted as an indirect proof that nickel is incorporated in the structure of this highly deformed dioxide. It should be noted that the thermal decomposition of nickel-free manganese carbonate precursor leads to α-Mn_2O_3 and cation deficient Mn_3O_4 solids as the mayor product in static air atmosphere between 400 and 1100°C [7]. Thus nickel is a requisite for the stabilisation of a (γ/β)-MnO_2-related structure by the precursor method.

According to previous research [1], a poor electrochemical lithium insertion behaviour is expected for γ-β structurally-related solids, having the diffraction patterns shown in Fig. 1, specially without previous modification with lithium nitrate. However, the SPES data recorded in Fig. 2 show significant discrepancies with the cycling behaviour

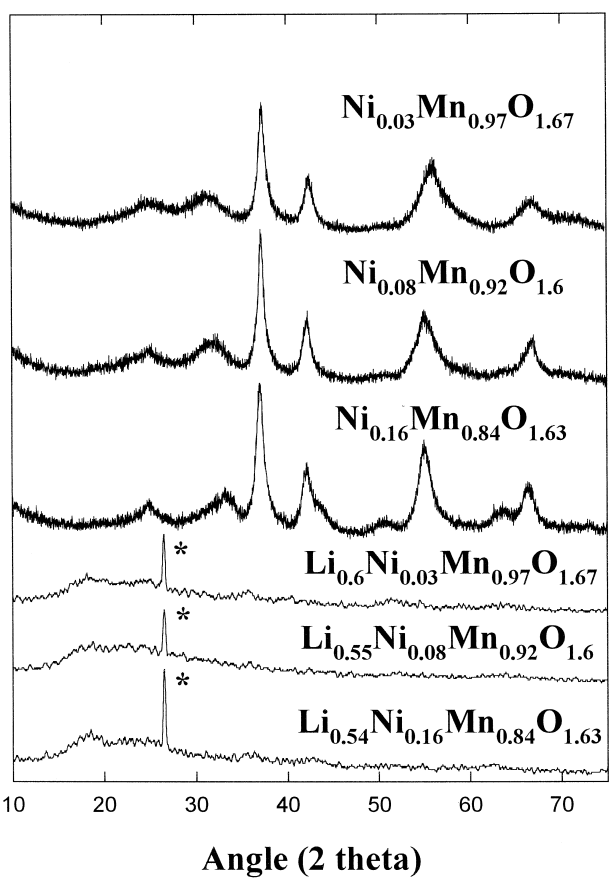

Fig. 1. X-ray diffraction patterns of the three pristine samples and electrochemically inserted products. * graphite additives.

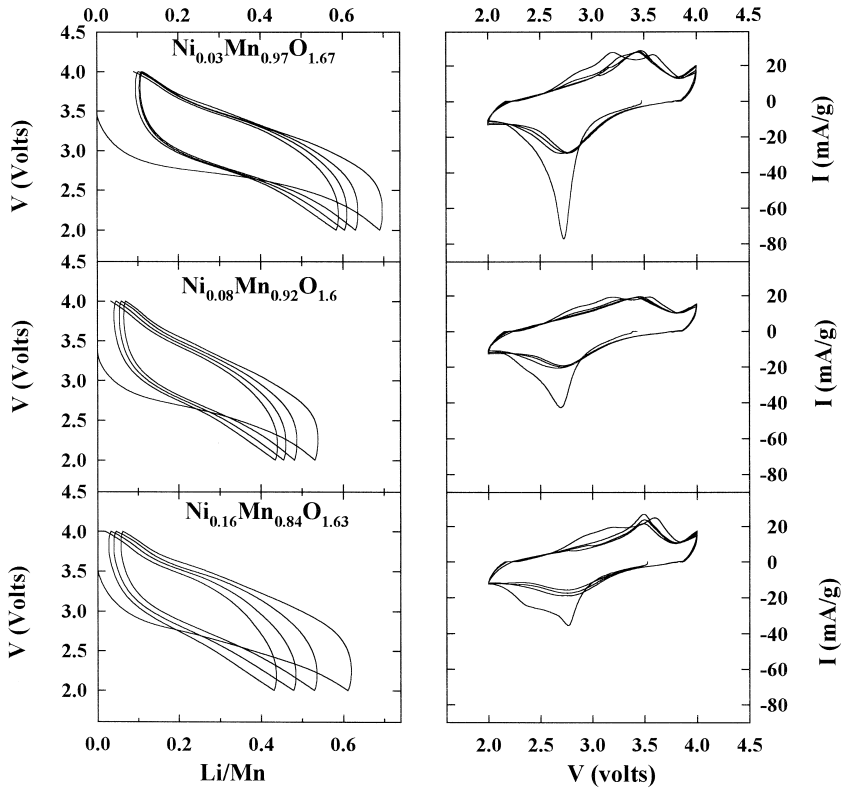

Fig. 2. Step potential electrochemical spectroscopy results of lithium cells using nickel-modified manganese oxides as active electrode material.

reported for nickel-free CMD and EMD [1,5,6]. Thus, the extent of the insertion process, expressed as Li/Mn ratio is larger than those previously reported [1]. Also, the effects found in the plot of cell current vs. voltage (Fig. 2) show additional complexity to the cyclic voltammograms previously reported [5]. In this way, the first cycle of discharge–charge leads to several peaks. Besides the intense reduction signal observed during the first discharge which is located at 2.8 V, a shoulder develops at ca. 2.4 V. The origin of these peaks can be associated to either different oxidation states involved in the reduction process (mainly Mn^{4+}/Mn^{3+} and Mn^{3+}/Mn^{2+} pairs), or to the different sites that can be used to accommodate lithium during cell discharge. The hysteresis observed during the first cycle is indicative of the second interpretation, as structural changes take place, as shown below. Also, the possible involvement of nickel in the shoulder at 2.4 V cannot be discarded. In fact, Tarascon et al. [10] suggested that a plateau occurring at 2.2 V during the first discharge of cells using Ni-substituted spinel electrodes could be due to the Ni possibly affecting the spinel structure. Moreover, although Ni^{3+} was not detected in related Mn^{4+}-containing systems [9–12], at present we have no direct evidence that all nickel is in the 2 + oxidation state in our modified oxides, and the possibility of a reduction of nickel during cell discharge cannot be completely discarded.

In addition, SPES data reveal a decrease in the intensity of the shoulder as nickel content decreases. As Ni is not expected to be involved in the reduction peaks observed during cell discharge, the different voltages at which lithium insertion/deinsertion take place can be associated with the different environments in which the insertion sites are located, including the number and distance of the neighbour nickel ions.

During the first cell charge, the shoulder and the main reduction peak lead to related oxidation signals although less intense and displaced to larger voltages, probably by kinetic effects. Thus, the main oxidation occurs at 3.3 V, while the shoulder is at ca. 2.7 V. In addition, a third well-defined peak develops at ca. 3.6 V, which increases its intensity with nickel content. This peak is not correlated with any reduction effect during cell discharge, even when the second cycle is considered. The nature of this oxidation effect leading to the hysteresis phenomenon should involve new and irreversible structural changes which lead to the new shape of the second cycle profile. Nevertheless, the possible participation of changes in the oxidation states during cell charge cannot be discarded.

The structural changes induced during the first discharge–charge cycle on the solids were monitored by X-ray diffraction. Only weak and highly broadened signals are shown in the patterns collected in the lower part of Fig. 1, which evidences a significant decrease in long range ordering.

The interest of the amorphization effect on the performance is also evident in the potentiostatic plots of Fig. 2.

A marked improvement is observed from the first to the second and following cycles: lower polarization, less marked hysteresis and better capacity retention.

Fig. 3 shows the changes in cell capacity during the first ten cycles. After a decrease in capacity, a good capacity retention is found during the following cycles. Moreover the enhanced lithium ion diffusivity in the cycled material can be observed in Fig. 4. The D values were computed according to the methodology reported by Weppner and Huggins [14]. Using the long step PITT relaxations which fulfilled the condition $t \gg L^2/10\ D$, plots of $\log(|i|)$ vs. t were obtained. The slope of these plots is simply $-1.071\ DL^2$. The average values of D are high as compared with lithium insertion into other manganese oxide electrodes [6]. A particular feature of the plots in Fig. 4 is the occurrence of a minimum in the values of the diffusion coefficients as a function of the discharge depth. This minimum is more marked for the lower nickel content and is almost absent for the Ni-rich composition. Its intensity agrees well with the intensity of the main reduction peaks in the SPES spectra of Fig. 2. The evolution contrasts with what is expected from a progressive filling of all the available sites in the structure of the oxide and the continuous increase in the interionic repulsions inside the structure of the host on increasing the degree of intercalation. The increase in D after the minimum implies a dramatic structural change which makes the solid adapted to the larger lithium content and allows a better diffusivity, e.g., by the incomplete amorphization. On average to the complete x interval, the higher coefficients are obtained for the higher nickel content. It should be remembered that the presence of such a small amount of nickel is a prerequisite for the stabilization of the pristine oxide structure and this behaviour comparable to that of $LiNO_3$ modified compositions (CDMO). For further discharges, the differences between samples are less marked (Fig. 4b).

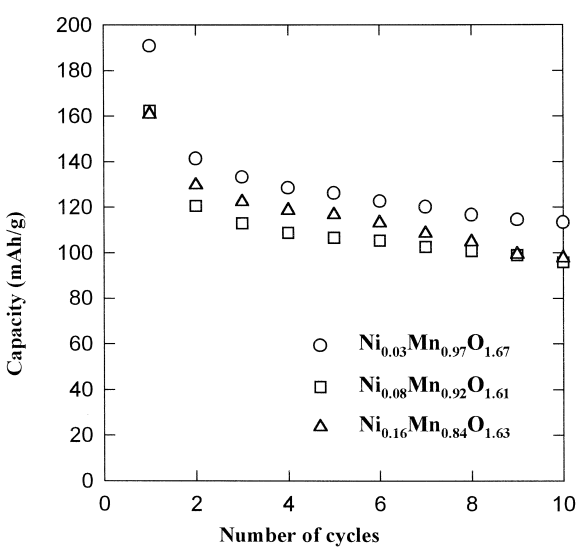

Fig. 3. Changes in cell capacity during the prolonged cycling of lithium cells.

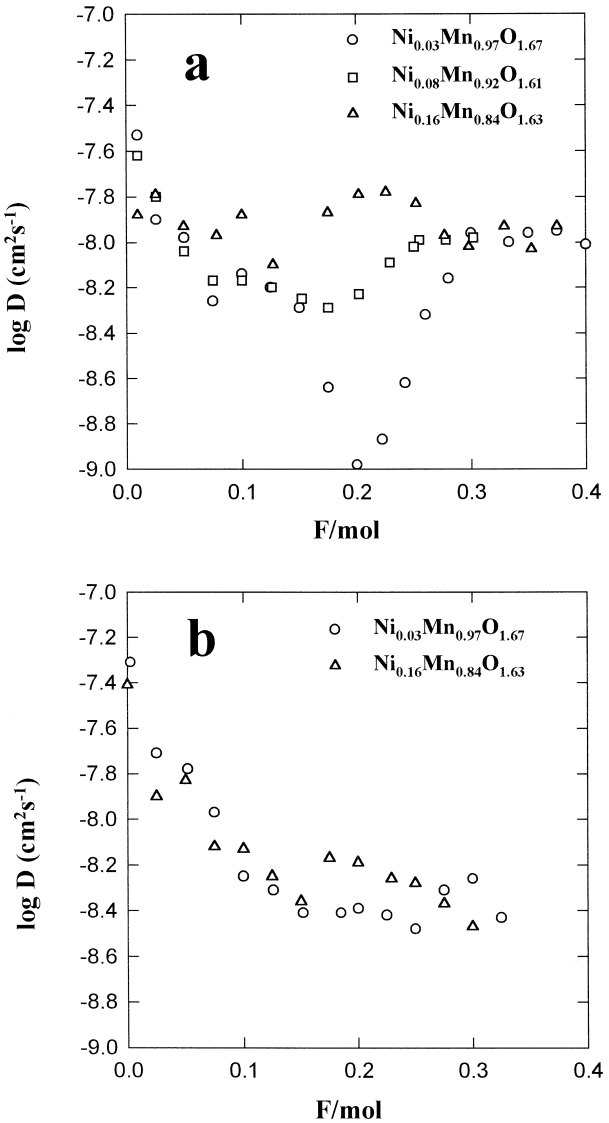

Fig. 4. Chemical diffusion coefficient during (a) first, and (b) second cell discharge.

In conclusion, the use of nickel containing composite manganese oxides leads to a simple synthetic route for the stabilization of this phases by using the carbonate precursor procedure. The lithium insertion–deinsertion cycles of this material vs. a lithium electrode reveal an interesting behaviour, without previous modification with lithium salts, as used in the past by different authors. From the point of view of its application in lithium cells, the low toxicity of manganese compounds is usually taken as one of the clear advantages of these solids vs. other solids such as V_2O_5. Also, nickel is less expensive and contaminant than other additives such as cobalt. The low temperature synthesis proposed here is economically interesting for the industrial production of the active cathode material.

Acknowledgements

The authors acknowledge financial support from the French and Spanish governments through the PICASSO program (contract HF 1997-0030).

References

[1] T. Nohma, S. Yoshimura, K. Nishio, T. Saito, in: G. Pistoia (Ed.), Lithium Batteries, Elsevier, New York, 1994, pp. 417–456.
[2] Sony's Lithium Manganese Rechargeable Battery, JEC Battery Newsletter 1, 1988, p. 26.
[3] Sanyo's Lithium Rechargeable Battery, JEC Battery Newsletter 1, 1989, p. 15.
[4] T. Nohma, T. Saito, N. Furukawa, H. Ikada, J. Power Sources 26 (1989) 389.
[5] L. Li, G. Pistoia, Solid State Ionics 47 (1991) 231.
[6] L. Li, G. Pistoia, Solid State Ionics 47 (1991) 241.
[7] J.M. Jiménez-Mateos, W. Jones, J. Morales, J.L. Tirado, J. Solid State Chem. 93 (1991) 443.
[8] L. Sánchez, J.L. Tirado, J. Electrochem. Soc. 144 (1997) 1939.
[9] K. Amine, H. Tukamoto, H. Yasuda, Y. Fujita, J. Electrochem. Soc. 143 (1996) 1607.
[10] J.M. Tarascon, E. Wang, F.K. Shokooki, W.R. McKinnon, S. Colson, J. Electrochem. Soc. 138 (1991) 2859.
[11] L. Guohua, H. Ikuta, T. Uchida, M. Wakihara, J. Electrochem. Soc. 143 (1996) 178.
[12] G. Pistoia, A. Antonini, R. Rosati, C. Bellitto, G.M. Ingo, Chem. Mater. 9 (1997) 1443.
[13] L. Christel, A. Pierre, D.A.M.R. Abel, Thermochim. Acta 306 (1997) 51.
[14] W. Weppner, R.A. Huggins, Ann. Rev. Mater. Sci. 8 (1978) 269.